Inhibition of F_1-ATPase from *Trypanosoma brucei* by its regulatory protein inhibitor $TbIF_1$

Ondřej Gahura[1,2], Brian Panicucci[1], Hana Váchová[1#], John E. Walker[2], Alena Zíková[1,3*]

[1]Institute of Parasitology, Biology Centre Czech Academy of Science, České Budějovice, Czech Republic;

[2]The Medical Research Council Mitochondrial Biology Unit, University of Cambridge, Cambridge Biomedical Campus, Hills Road, Cambridge CB2 0XY, United Kingdom;

[3]Faculty of Science, University of South Bohemia, Ceske Budejovice, Czech Republic

#To whom correspondence should be addressed: Alena Zíková, Institute of Parasitology, Biology Centre Czech Academy of Science, Branišovská 31, 37005, České Budějovice, Czech Republic; Tel.: 0042038775482; Email: azikova@paru.cas.cz; website: http://www.paru.cas.cz/en

[*]Present address: Institute of Molecular Biology, Czech Academy of Science, Prague, Czech Republic.

Running title: *Inhibition of F_1-ATPase in Trypanosoma brucei*

Abbreviations: I1-60, monomeric form of bovine IF_1, consisting of residues 1 to 60; PF, procyclic form; BF, bloodstream form; k_{on}, rate constant of inhibitor's binding; k_{off}, rate constant of inhibitor's dissociation; K_i, dissociation constant of the inhibitor-enzyme complex

Key words: F_1F_o-ATPase, trypanosome, *Trypanosoma brucei*, ATP synthase, enzyme inhibitor, F-ATPase, IF_1, $TbIF_1$

Conflict of interest:

The authors declare there is no conflict of interest associated with the manuscript.

ABSTRACT

Hydrolysis of ATP by the mitochondrial F-ATPase is inhibited by a protein called IF_1. In the parasitic flagellate, *Trypanosoma brucei*, this protein, known as $TbIF_1$, is expressed exclusively in the procyclic stage, where the F-ATPase is synthesizing ATP. In the bloodstream stage, where $TbIF_1$ is absent, the F-ATPase hydrolyzes ATP made by glycolysis and compensates for the absence of a proton pumping respiratory chain by translocating protons into the intermembrane space, thereby maintaining the essential mitochondrial membrane potential. We have defined regions and amino acid residues of $TbIF_1$ that are required for its inhibitory activity by analyzing the binding of several modified recombinant inhibitors to F_1-ATPase isolated from the procyclic stage of *T. brucei*. Kinetic measurements revealed that the C-terminal portion of $TbIF_1$ facilitates homodimerization, but it is not required for the inhibitory activity, similar to the bovine and yeast orthologs. However, in contrast to bovine IF_1, the inhibitory capacity of the C-terminally truncated $TbIF_1$ diminishes with decreasing pH, similar to full length $TbIF_1$. This effect does not involve the dimerization of active dimers to form inactive tetramers. Over a wide pH range, the full length and C-terminally truncated $TbIF_1$ form dimers and monomers, respectively. $TbIF_1$ has no effect on bovine F_1-ATPase, and this difference in the mechanism of regulation of the F-ATPase between the host and the parasite could be exploited in the design of drugs to combat human and animal African trypanosomiases.

INTRODUCTION

Most eukaryotic cells use the mitochondrial electron transport chain and oxidative phosphorylation to generate ATP under aerobic conditions. The production of ATP is catalyzed by the terminal enzyme of the oxidative phosphorylation pathway, the F-ATPase (also called F_1F_o-ATPase or ATP synthase). Together with respiratory enzyme complexes I, II, III and IV, the F-ATPase is located in the inner mitochondrial membrane where it uses the electrochemical potential difference for protons across the membrane generated by complexes I, III and IV. The proton flux from the intermembrane space, through the membrane domain of the F-ATPase, into the mitochondrial matrix, drives the turning of the enzyme's rotor. The rotor is

composed of a ring of c-subunits in the membrane sector of the enzyme, attached to an elongated central stalk, which lies along the six-fold axis of pseudo-symmetry in the membrane-extrinsic F_1-catalytic domain. This rotation drives the sequential binding of substrates ADP and phosphate and the formation of ATP in each of the three catalytic sites, which are found at interfaces between α- and β-subunits in the F_1-domain (for reviews see [1, 2]). The enzyme can also act in reverse to hydrolyze ATP, changing the direction of rotation of the rotor, and pumping protons from the mitochondrial matrix into the intermembrane space. Under certain conditions, for example during anoxia, this reverse mechanism counteracts the depolarization of the inner mitochondrial membrane. However, in order to minimize the risk of deleterious depletion of ATP, this proton translocation at the expense of ATP is tightly regulated [3] by a mechanism involving an inhibitor protein, known as IF_1. This protein is found throughout eukarya, and has been studied mainly in bovine, human and yeast mitochondria. The bovine protein is a potent unidirectional inhibitor of the ATP hydrolytic activity of the F-ATPase, without effect on the synthesis of ATP [4, 5]. The active form of bovine IF_1 is a dimer where the monomers are held together by an α-helical coiled-coil in the C-terminal regions of the two protein monomers. In the free dimeric inhibitor, near neutral pH, the N-terminal inhibitory region is intrinsically unfolded, whereas under slightly alkaline conditions (ca. pH 8.0), IF_1 becomes inactive by formation of dimers of dimers and higher aggregates that mask the inhibitory region [6, 7]. The formation of the fully inhibited state of the ATPase requires the hydrolysis of two ATP molecules. In the structure of the bovine F_1-ATPase inhibited by a monomeric form of IF_1 (known as I1-60 and consisting of the residues 1-60), the largely α-helical N-terminal region of the inhibitor is bound in a deep groove at the most closed of the three catalytic interfaces of bovine F_1-ATPase. Here, it makes contacts with five of the nine subunits of the enzyme [8]. In the presence of a large molar excess of either unmodified I1-60 or a mutated monomeric form carrying the mutation K39A, the inhibited F_1-ATPase complex has two or three molecules of IF_1 bound at catalytic interfaces. These complexes represent intermediate stages in the binding of IF_1 to F_1-ATPase in the pathway from the unbound and unfolded inhibitory region to the progressively folded and final fully folded inhibited state of F_1-ATPase [9]. The inhibitor protein from *Saccharomyces cerevisiae* binds to yeast F_1-ATPase in a closely similar manner to the binding of bovine IF_1 to bovine F_1-ATPase

[10]. Moreover, bovine IF_1 is an effective inhibitor of yeast F_1-ATPase and *vice versa* [11, 12]. However, yeast IF_1 is monomeric, not dimeric, as it lacks the C-terminal dimerization domain, and so its activity is not regulated by the formation of higher oligomers [12, 13]. In human mitochondria, IF_1 has been reported to protect cardiac tissue against the loss of ATP during ischemia [14, 15], has been linked to anti-apoptotic activity and oncogenesis in various cell lines and tissues [16, 17], and has been proposed to play an important role in the *in vivo* process of assembly of ATP synthase, by acting to prevent partially assembled complexes with the capability to hydrolyze ATP from doing so [18].

The parasitic flagellate, *Trypanosoma brucei* is the causative agent of sleeping sickness. It has a complex life cycle including two main proliferative stages, the procyclic form (PF) in the tsetse fly (*Glossina* sp.) and the bloodstream form (BF) in the final mammalian host [19]. As these two stages occur in entirely different environments, they differ fundamentally in cell morphology and physiology, including their mechanisms of energy conversion [20]. In the PF, ATP is produced mostly by oxidative phosphorylation where the F-ATPase generates ATP [21]. In contrast, the BF is supplied by virtually unlimited glucose from the blood of the host, and ATP is provided by glycolysis. The BF mitochondria are devoid of respiratory complexes III and IV, and complex I is non-essential and dispensable. Instead, reducing equivalents are channeled via the alternative NADH dehydrogenase, and the electrons are transferred to oxygen by the non-proton pumping alternative oxidase (for reviews see [22, 23]). The essential mitochondrial membrane potential is maintained by the proton pumping activity of the F-ATPase driven by the hydrolysis of ATP [24, 25]. The genome of *T. brucei* encodes an ATPase inhibitor protein known as $TbIF_1$. However, as expected, it is expressed only in PF cells. Ectopic expression of $TbIF_1$ in the BF stage causes the collapse of the mitochondrial membrane potential and a rapid inhibition of growth [26].

As described below, we have characterized $TbIF_1$ and its binding *in vitro* to its cognate F_1-ATPase. We have defined the regions of $TbIF_1$ that are essential for the inhibitory activity. We have compared the sensitivity of its activity to pH, and its ability to form homo-oligomers with the bovine ortholog, and demonstrated that $TbIF_1$ is incapable of inhibiting the bovine enzyme. Therefore, since the hydrolytic

activity of the F-ATPase is absolutely required in the BF of *T. brucei*, compounds mimicking the action of $TbIF_1$ could be developed to selectively inhibit the parasite F-ATPase without affecting the human enzyme as new therapies for the treatment of sleeping sickness and related African trypanosomiases.

RESULTS AND DISCUSSION

Characterization of $TbIF_1$ and variants

In order to characterize $TbIF_1$ and to study how its features are involved in the inhibition of F_1-ATPase in *T. brucei*, several variants of $TbIF_1$ were expressed in *Escherichia coli* without the N-terminal mitochondrial targeting sequence (Fig. 1A) and with a C-terminal 6xHis tag used in their purification by affinity chromatography. The proteins include the intact mature $TbIF_1$ from residues 1-93 and named $TbIF_1$-WT, a C-terminally truncated version, $TbIF_1$(1-64), N-terminally truncated versions $TbIF_1$-Δ1-5, -Δ1-8, -Δ1-10, -Δ1-12 and -Δ1-15, and full-length forms with point mutations, $TbIF_1$(E24A), $TbIF_1$(E27A), $TbIF_1$(P32A) and $TbIF_1$(Y24W). The purity of the isolated proteins was demonstrated by analysis by SDS-PAGE (Fig. 1B), and their sequences were verified by measurement of their intact molecular masses (Table S1). The choice of these mutated forms of $TbIF_1$ was based upon knowledge of the mode of action of the bovine and yeast inhibitor proteins, and on sequence relationships between these proteins and other orthologs with $TbIF_1$ (Fig. 1A). This sequence alignment demonstrates that the inhibitory region from residues 19-59 is well conserved, especially from residues F25 to L48, which forms the α-helical region that interacts with F_1-ATPase in the bovine and yeast enzymes, except that residues R25, A28, F34, A43, and A44 [27], identified as being critical for the binding of bovine IF_1 to its cognate F_1-ATPase, are not conserved in $TbIF_1$ (Table S2).

The N-terminal inhibitory domain of the bovine IF_1 is intrinsically disordered and becomes progressively structured in the process of binding to F_1-ATPase [9]. The CD spectrum of $TbIF_1$-WT is typical of a protein with high α-helical content [28], whereas the spectrum of $TbIF_1$(1-64) is typical of a random structure (Fig. 1C). Thus, it appears that the conserved N-terminal part of $TbIF_1$ is intrinsically unfolded, as in bovine IF_1, and the α-helical component of the CD spectrum comes from the C-terminal

region where residues 33-93 are predicted to form a single α-helix (Fig. 1A) with the potential to form an anti-parallel α-helical coiled-coil (residues 60-93), as in bovine IF_1 [29].

In contrast to the conservation of the sequence of residues 25-88, residues 1-24 of $TbIF_1$ are largely unconserved. The region from residues 1-18 is predicted to be unstructured, and the regions from 19-27 and 33-93 to be α-helical. In the bovine enzyme, the N-terminal region from residues 1-13 is also unstructured and makes contact the α_E-subunit. Residues 14-18 form a short α-helix which is in contact with the N-terminal α-helix of the γ-subunit [8, 10], thereby contributing to the strength of the interaction between the enzyme and the inhibitor [27]. The sequence alignment also revealed a stretch of residues starting at I49 of $TbIF_1$, which appears to be specific for kinetoplastids (Fig. 1A).

Oligomerization of $TbIF_1$

The ability of $TbIF_1$ to form homo-oligomers was examined by two independent approaches. It was demonstrated by covalent cross-linking with dimethylsuberimidate that, similar to the bovine protein, $TbIF_1$-WT forms dimers at pH values above neutrality, whereas $TbIF_1$(1-64) did not (Fig. 2A). However, the higher oligomers observed with the bovine protein were not formed by $TbIF_1$-WT. The oligomerization state was examined also by gel filtration chromatography (Table 1 and Fig. 2B). With the control samples, monomeric bovine I1-60 and full length bovine IF_1, the values obtained at pH 8.0 were approximately twice those expected for monomers and dimers, probably in consequence of the dimers consisting of a partly of an antiparallel α-helical coiled coil structure approximately 130 Å long involving residues 19-81, with a disordered structure from residues 1-18 extending in opposite directions from each monomer [7]. The values obtained with $TbIF_1$-WT and $TbIF_1$(1-64) were similarly greater than expected from their calculated molecular masses. By comparison with the bovine values, and assuming that $TbIF_1$ has a similar overall structure to bovine IF_1, which the sequence similarities suggest, the observed values are consistent with $TbIF_1$(1-64) being monomeric, and the formation of dimers by $TbIF_1$ both above and below neutral pH. In contrast to the bovine protein, $TbIF_1$ appears not to form oligomers greater than dimers under any of the conditions that were investigated. Therefore, it appears that in contrast to bovine IF_1, where the transition

from the active dimeric state to the inactive tetrameric and higher oligomeric states is governed by pH [6], $TbIF_1$ does not form dimers of dimers and higher oligomers at pH 8.0, and there is no evidence for a pH regulated active-inactive switch with $TbIF_1$.

Influence of pH and the C-terminal region of $TbIF_1$ on its inhibitory activity

The kinetics of the inhibition of F_1-ATPase by $TbIF_1$ were characterized by measurement of the rate constants of the inhibitor's binding (k_{on}) and dissociation (k_{off}), and the dissociation constant of the inhibitor-enzyme complex (K_i). The kinetic measurements were carried out with F_1-ATPase isolated from the procyclic form of *T. brucei* [30]. These kinetic data are summarized in Table 2. In contrast to bovine IF_1 where the C-terminally truncated variant has a higher inhibitory potential than the intact protein at pH 8.0 [6], K_i, k_{on} and k_{off} do not differ between intact $TbIF_1$ and $TbIF_1$(1-64). This difference is unsurprising as $TbIF_1$ does not form tetramers, which is facilitated by the C-terminal part of IF_1 in the bovine protein [7]. Reduction of the pH to 6.5 is accompanied by a significant increase in the affinity of $TbIF_1$ for F_1-ATPase (Table 2). In mammals, a similar phenomenon is explained by the need to prevent ATP depletion by hydrolysis by F-ATPase, accompanying membrane depolarization and acidification of the matrix [31]. The increased affinity of IF_1 affinity counteracts this hydrolysis and helps to maintain sufficient levels of ATP [32]. A similar mechanism may operate also in *T. brucei* during hypoxia [26]. At pH values of both 8.0 and 6.5, the deletion of C-terminus does not affect the binding of the inhibitor to F_1-ATPase. Approximately two-fold decrease in k_{off} and ten-fold increase in k_{on} contributed to a lower value of K_i at pH 6.5 in comparison to pH 8.0 (Table 2), indicating that the inhibitor binds to the enzyme at a higher rate and, in addition, the inhibited complex is more stable under these conditions.

The ability of $TbIF_1$ to inhibit F_1-ATPase could either increase gradually with decreasing pH or it could change sharply at a certain threshold pH value. To distinguish between these two possibilities, the purified F_1-ATPase was inhibited with either intact $TbIF_1$ or $TbIF_1$(1-64) at pH values from 6.0-9.0 and residual ATPase activities were measured. The response of $TbIF_1$ inhibitory potential to pH change was gradual and had no threshold (Fig. 3). Also, as expected, the lack of the C-terminal region of $TbIF_1$ had no

effect on the inhibition F_1-ATPase over a range of pH values, and for both intact and truncated $TbIF_1$, the residual activities were very similar, consistent with the C-terminal part of $TbIF_1$ not being involved directly in the interaction with F_1-ATPase, as in other species [8, 10].

Effect of truncation of the N-terminal region of $TbIF_1$

The inhibitory capacities of $TbIF_1$-Δ1-5, -Δ1-8, -Δ1-10, -Δ1-12 and -Δ1-15 were compared with full length $TbIF_1$. It was confirmed that the inhibitory effect of intact $TbIF_1$ is greater at pH 6.5 than at pH 8.0, and that at pH 6.5 a concentration of 0.1 μM is more effective than the same concentration at pH 8.0 (Fig. 4A). Removal of the N-terminal region of $TbIF_1$ up to residue 10, had no effect on the inhibitory capacity of $TbIF_1$, but removal of residues 1-12 and 1-15, impaired the inhibitory capacity of the protein progressively (Fig. 4B). Thus, the region in the vicinity of residues 14-16 defines the N-terminal extremity of the minimal inhibitory sequence of $TbIF_1$. At pH 8.0, the inhibitory capacities of all the truncated versions followed the same trend as at pH 6.5, except that the inhibitory capacities were lower (not shown), suggesting that the N-terminal region of $TbIF_1$ from residues 1-16 does not participate in the effects of pH on inhibitory activity.

In the structure of bovine F_1-ATPase inhibited by IF_1, residues 1-7 of IF_1 were not resolved and residues 8-13 have an extended structure [8]. Thus, the increased entropy of this region may destabilize the interaction of the enzyme with the inhibitor [27]. In the bovine inhibited complex, residues 14-18 form a short α-helix, followed by a short loop from residues 19-21 which interacts with the N-terminal α-helix in the α-helical coiled-coil region of the γ-subunit. Despite the lack of conservation of this region of the sequence of the inhibitor protein in *S. cerevisiae* (Fig. 1A), the yeast IF_1 interacts with its cognate F_1-ATPase in a similar way [10]. The sequences of the N-terminal regions of $TbIF_1$ and bovine IF_1 also differ extensively (Fig. 1A), and yet deletion of this region has a similar impact on their inhibitory capacities [27]. Therefore, as in the bovine and yeast inhibited complexes, it seems likely that in the complex of TbF_1-ATPase inhibited by $TbIF_1$, the N-terminal region of $TbIF_1$ will interact with TbF_1-ATPase in a similar way to the mode of interaction of the bovine and yeast IF_1 proteins with their cognate F_1-ATPases.

Effects of point mutations of $TbIF_1$ on inhibition of F_1-ATPase

The N-terminal inhibitory domain of IF_1 contains several residues that are strictly conserved in mammals, fungi and kinetoplastids (Fig. 1A). This conservation suggests that they have a general role in the action of IF_1, either directly by participating in the interaction between IF_1 and F_1-ATPase or indirectly in the process of formation of the inhibited complex, which is complicated by the requirement to fold the inhibitory region from its intrinsically disordered unbound state [9]. Introduction of the mutation Y36W into the conserved residue Tyr-36 of $TbIF_1$ increased the inhibitory potency of $TbIF_1$ (Fig 4C). This observation is consistent with the conservation of Asp-394 and Lys-401 in the β-subunit, which interact with Tyr-33 in the bovine inhibited complex (Table S2 and [8, 9]).

In bovine inhibited complex, residues 21-46 of the long α-helix of IF_1 are strictly or conservatively conserved in 14 out of 26 residues in comparison to $TbIF_1$, but not residue Pro-32, which replaces Glu-28 in bovine IF_1. In addition to being unconserved, Glu-28 is not in contact with F_1-ATPase in the inhibited complex. The introduction of a proline residue might be expected to change the secondary structure of $TbIF_1$ by breaking the long α-helix. However, the substitution of this residue by alanine in $TbIF_1$(P32A) had only a slight effect on the inhibitory capacity of $TbIF_1$ (Fig. 4C), and so it appears likely that this proline residue has only a minor structural effect on $TbIF_1$, possibly introducing a kink in the long α-helix rather than changing its secondary structure radically. As expected, the mutation $TbIF_1$(P32A) had no effect on the α-helical content of $TbIF_1$ alone, as this region of the protein is presumably disordered as in the unbound bovine IF_1 (Fig. 1C).

Similar to bovine IF_1 and IF_1 in *S. cerevisiae*, the inhibitory activity of $TbIF_1$ is pH dependent (Fig. 3) [13]. It has been proposed that in the yeast protein, this pH dependence involves Glu-21 (residue 30 in the aligned sequences in Fig. 1A). However, this glutamate residue is not conserved in kinetoplastids, and adjacent residues are also poorly conserved (Fig. 1A). Therefore, two other nearby glutamate residues at positions 24 and 27 were mutated separately to alanine, generating $TbIF_1$(E24A) and $TbIF_1$(E27A). However, neither mutation enhanced the inhibition of F_1-ATPase at pH 8.0, and their inhibitory capacity at

pH 6.5 remained the same as the inhibitory capacity of $TbIF_1$-WT (Fig. 4C). Thus, the sensitivity of the inhibitory potency of $TbIF_1$ to pH is explained neither by these point mutations, nor by a change in oligomerization state [6]. An explanation will need to be sought elsewhere.

Heterologous inhibitory effects of $TbIF_1$ and bovine IF_1

Bovine F_1-ATPase was hardly inhibited at all by $TbIF_1$, but bovine IF_1 had a significant inhibitory effect on the F_1-ATPase from *T. brucei*, albeit considerably less than by $TbIF_1$ (Fig. 5). In the current absence of structure of TbF_1-ATPase inhibited by $TbIF_1$, it is difficult to explain these observations in molecular terms. However, most of residues in the β-subunit of bovine F_1-ATPase involved in the interaction with bovine IF_1 [8, 9] are conserved in trypanosomes, whereas other interactions between bovine IF_1 with α- and γ-subunits are generally poorly conserved (Table S2). It is among these poorly conserved residues in α- and γ-subunits that an explanation may lie.

F_1-ATPase and $TbIF_1$ interaction interface as a drug target

In the BF of *T. brucei*, the membrane potential of their mitochondria is maintained by the hydrolysis of ATP by ATP synthase. The ATP molecules are supplied from the cytosol and are imported to the mitochondrial matrix by the ADP-ATP translocase. The survival of the parasite in the bloodstream depends on this mechanism [25,33]. Only recently has it been demonstrated that $TbIF_1$ suppresses the hypoxia-related mitochondrial membrane potential phenotype in the PF cells of *T. brucei*, and that *in vivo* $TbIF_1$ inhibits ATPase, but not ATP synthesis [26]. The experiments described here show common features and significant differences between $TbIF_1$ and the mammalian inhibitor protein. The inhibitors inhibit the hydrolytic activity of their cognate F_1-ATPases by probably binding to the enzyme in a similar way. However, they differ in their oligomeric state and in the regulation of their inhibitory activity by pH. Moreover, $TbIF_1$ has no effect on bovine F_1-ATPase, which is very similar in its structure and properties to the human enzyme. Therefore, it is conceivable that compounds mimicking the action of $TbIF_1$ could be developed to inhibit the ATP hydrolytic activity of the BF of *T. brucei*, leading potentially to new therapies

for the treatment of African trypanosomiases. Recently, the structure of the F_1-ATPase from *T. brucei* was described [34], and the development of such new therapeutic compounds would be greatly aided by an atomic resolution structure of the *T. brucei* F_1-ATPase inhibited by $TbIF_1$. The F-ATPase in *Mycobacterium tuberculosis* is an authenticated drug target for treatment of tuberculosis, and bedaquiline, an inhibitor of the enzyme, is now in clinical use [35,36]. The current findings open a possible pathway for the development of the F-ATPase in *T. brucei* as a drug target.

EXPERIMENTAL PROCEDURES

Cloning, expression, and purification of variants of $TbIF_1$

Fragments encoding truncated versions of $TbIF_1$ were amplified by PCR from genomic DNA from PF *T. brucei* Lister strain 427 with forward and reverse primers containing *Nde*I and *Hind*III restriction sites, respectively. All reverse primers encoded the hexahistidine tag (6xHis). The PCR products were inserted into the expression vector pRUN [37], pre-digested with *Nde*I and *Hind*III. Site-directed mutagenesis was carried out with a QuikChange Lightning mutagenesis kit (Agilent Technologies, USA). Oligonucleotides used in amplification and mutagenesis are listed in the Table S3. The sequences of cloned regions were verified by DNA sequencing. Plasmids were transformed into *Escherichia coli* C41(DE3) [38], and the cells were grown in LB medium. When the OD_{600} had reached ca. 0.4, the expression of the recombinant protein was induced by the addition of 1 mM isopropyl β-D-1-thiogalactopyranoside for 3 hours. Then the cells were harvested, washed in phosphate buffered saline, resuspended at 4°C in buffer containing 20 mM Tris-HCl, pH 7.4, 10% (w/v) glycerol, 100 mM NaCl and 25 mM imidazole supplemented with the cOmplete EDTA-free protease inhibitor cocktail (Roche, Switzerland). They were lysed with lysozyme (75 μg/ml) for 30 min at 4°C in the presence of DNase I (15 U/ml). The lysate was sonicated (5x20 s), and cooled on ice for 1 min between impulses, centrifuged (15000 x g, 30 min, 4°C), filtered (0.45 μm pores), and applied to a HisTrap nickel affinity column (GE Healthcare, United Kingdom) in the same buffer. The $TbIF_1$ variants were eluted with a 50 ml linear gradient of imidazole from 20-500 mM. Fractions were analyzed by SDS-PAGE. Those containing $TbIF_1$ were pooled and dialyzed against buffer containing 20

mM Tris-HCl, pH 7.4, and 10% glycerol (w/v), concentrated by membrane filtration (molecular weight cut-off 3.5 kDa, Sartorius, Germany) to 10-20 mg/ml, flash-frozen in liquid N_2, and stored at -80°C.

Purification of F_1-ATPase

F_1-ATPase from *T. brucei* was purified from PF strain 427 as described previously [30]. Its specific activity was determined as described below [39] and was 56 $\mu mol \times min^{-1} \times mg^{-1}$.

Protein analysis

The process of purification and the purity of recombinant $TbIF_1$ variants and F_1-ATPase were monitored by SDS-PAGE in the presence of Tris-glycine. Protein bands were stained with Coomassie Brilliant Blue. The molecular masses of $TbIF_1$ proteins were verified by liquid chromatography coupled to mass spectrometry (LC/MS) in a 4000 QTrap triple quadrupole mass spectrometer a (AB SCIEX, USA) equipped with electrospray ionization.

Protein cross-linking

Purified inhibitor proteins were dialyzed into buffer consisting of 20 mM HEPES and 1 mM EDTA, at various pH values, and then diluted to a concentration of 0.1 mg/ml. Dimethylsuberimidate (DMS) dissolved in water was added to give a final concentration of 1 mg/ml. After various periods, the reaction was terminated by mixing the samples with the loading buffer for SDS-PAGE. The cross-linked proteins were analyzed by SDS-PAGE on 15% gels and stained with Coomassie Brilliant Blue dye.

Analytical gel-filtration

Purified $TbIF_1$ and bovine IF_1, both at a concentration of 3 mg/ml, were dialyzed into buffers with various pH values: 20 mM Tris-HCl, pH 8.0 and 7.4, and 10 mM MOPS-NaOH, pH 6.5. All buffers contained 10% (w/v) glycerol and 150 mM NaCl. The samples were applied to a Superdex 75 10/300 GL gel-filtration

column (GE Healthcare, UK) equilibrated in the respective buffer, and calibrated with a gel filtration LMW Calibration Kit (GE Healthcare). The uv absorption of the eluate was recorded at 280 nm.

Assay of inhibition of F_1-ATPase

The activity of TbF_1-ATPase was measured with an ATP regenerating assay as described before [27,39]. For estimation of the inhibitory effects of $TbIF_1$, ATP hydrolysis by F_1-ATPase was initiated, and 15s later the inhibitor protein was introduced in buffer containing 20 mM Tris-HCl, pH 7.4 and 10% (w/v) glycerol, and the absorbance was recorded for 10 min. The initial exponential decay of the ATPase activity following inhibition is described by the equation:

$$y_t - y_0 = V_0 t + [(V_0 - V_\infty)/k_{inh}][1-\exp(-k_{inh} t)] \quad (1)$$

where y_t is absorbance at time t, y_0 is absorbance at the point of inhibitor addition, V_0 is the initial rate of the reaction before the addition of inhibitor, V_∞ is rate of reaction at equilibrium, and k_{inh} is the apparent inhibitory constant. In the presence of a large molar excess of the inhibitor over the enzyme, the reaction can be assessed as pseudo-first order, and k_{inh}, expressed in reciprocal seconds (s^{-1}), is directly proportional to the concentration of inhibitor ([I]):

$$k_{inh} = k_{on}[I] + k_{off} \quad (2)$$

Therefore, the slope of the linear regression of k_{inh} plotted against [I] corresponds to the rate constant of the binding of the inhibitor, k_{on}, expressed as $\mu M^{-1}s^{-1}$. To obtain K_i, the dissociation constant of the inhibitor binding to the enzyme complex, expressed as μM, the ratio of final and initial reaction rates (V_∞/V_0) was fitted to the equation:

$$V_\infty/V_0 = v_{ins} + (1-v_{ins})/(1+[I]/K_i) \quad (3)$$

where v_{ins} is the inhibitor insensitive fraction of the initial rate of reaction; its value was set to the proportion of the initial ATPase activity which cannot be inhibited by the specific F_1-ATPase inhibitor sodium azide. The rate constant of inhibitor dissociation, k_{off}, expressed as s^{-1}, was calculated directly from the following relationship derived from equations (2) and (3):

$$V_\infty/V_0 = v_{ins} + [(1-v_{ins})k_{off}](1/k_{inh}) \quad (4)$$

Theoretically, k_{off} is given also by the intercept of the *y* axis of equation (2). However, the approach using equation (4) is independent of [I], which eliminates any impact of possible inaccuracies in the concentrations of inhibitor solutions. An example of data processing and calculations is shown in Fig. S1.

To measure the residual F_1-ATPase activity in equilibrium with different inhibitor variants, F_1-ATPase was mixed with the inhibitor in 500 µl of assay mixture lacking NADH, phosphoenolpyruvate, pyruvate kinase and lactate dehydrogenase. After 5 min at 37°C, when equilibrium had been reached, a further 500 µl of reaction mixture containing at twice their normal concentrations of constituents to compensate for their absence in the first half of the mixture were added, and the linear decrease of absorbance was recorded for 60 s. The residual ATPase activity was calculated as the ratio of decrease of absorbance in the presence and absence of inhibitor.

Circular dichroism

Mutated forms of $TbIF_1$ were dialyzed into buffer consisting of 100 mM sodium phosphate, pH 8.0 or 6.5, 10% (w/v) glycerol, and diluted to a concentration of 0.125 mg/ml. The circular dichroism spectra were recorded from 190-240 nm in a Jasco J715 instrument.

Bioinformatic analysis

The mitochondrial import sequence of $TbIF_1$ was predicted with MitoProtII [40].

Acknowledgements

This work was supported by the Ministry of Education ERC CZ grant LL1205 and Grant Agency of the Czech Republic (18-17529S) (both to A.Z.), by European Regional Development Fund (No. CZ.02.1.01/0.0/0.0/16_019/0000759), and by the Medical Research Council of the United Kingdom by Grant 21 522 MC_U1065663150 and by Programme Grant MR/M009858/1 (both to J. E. W.). We thank Drs J. V. Bason and R. Litvín for help with the kinetic analyses and measurement of CD spectra, respectively.

Contributions of authors:

AZ and JEW conceived and supervised the study. OG, AZ, BP and JEW designed the experiments, and OG performed the experiments. HV cloned, expressed and purified recombinant inhibitor proteins. AZ, OG, BP and JEW wrote the paper.

References

1. Walker, J. E. (2013) The ATP synthase: the understood, the uncertain and the unknown, *Biochem Soc Trans.* **41**, 1-16.
2. Walker, J. E. (2017) Structure, Mechanism and Regulation of ATP Synthases in (Wikstrom, M., ed), The Royal Society of Chemistry.
3. St-Pierre, J., Brand, M. D. & Boutilier, R. G. (2000) Mitochondria as ATP consumers: cellular treason in anoxia, *Proc Natl Acad Sci U S A.* **97**, 8670-4.
4. Pullman, M. E. & Monroy, G. C. (1963) A Naturally Occurring Inhibitor of Mitochondrial Adenosine Triphosphatase, *J Biol Chem.* **238**, 3762-9.
5. Runswick, M. J., Bason, J. V., Montgomery, M. G., Robinson, G. C., Fearnley, I. M. & Walker, J. E. (2013) The affinity purification and characterization of ATP synthase complexes from mitochondria, *Open Biol.* **3**, 120160.
6. Cabezon, E., Butler, P. J., Runswick, M. J. & Walker, J. E. (2000) Modulation of the oligomerization state of the bovine F_1-ATPase inhibitor protein, IF_1, by pH, *J Biol Chem.* **275**, 25460-4.
7. Cabezon, E., Runswick, M. J., Leslie, A. G. & Walker, J. E. (2001) The structure of bovine IF_1, the regulatory subunit of mitochondrial F-ATPase, *EMBO J.* **20**, 6990-6.
8. Gledhill, J. R., Montgomery, M. G., Leslie, A. G. & Walker, J. E. (2007) How the regulatory protein, IF_1, inhibits F_1-ATPase from bovine mitochondria, *Proc Natl Acad Sci U S A.* **104**, 15671-6.
9. Bason, J. V., Montgomery, M. G., Leslie, A. G. & Walker, J. E. (2014) Pathway of binding of the intrinsically disordered mitochondrial inhibitor protein to F_1-ATPase, *Proc Natl Acad Sci U S A.* **111**, 11305-10.
10. Robinson, G. C., Bason, J. V., Montgomery, M. G., Fearnley, I. M., Mueller, D. M., Leslie, A. G. & Walker, J. E. (2013) The structure of F_1-ATPase from *Saccharomyces cerevisiae* inhibited by its regulatory protein IF_1, *Open Biol.* **3**, 120164.
11. Satre, M., de Jerphanion, M. B., Huet, J. & Vignais, P. V. (1975) ATPase inhibitor from yeast mitochondria. Purification and properties, *Biochim Biophys Acta.* **387**, 241-55.
12. Cabezon, E., Butler, P. J., Runswick, M. J., Carbajo, R. J. & Walker, J. E. (2002) Homologous and heterologous inhibitory effects of ATPase inhibitor proteins on F-ATPases, *J Biol Chem.* **277**, 41334-41.
13. Ichikawa, N., Karaki, A., Kawabata, M., Ushida, S., Mizushima, M. & Hashimoto, T. (2001) The region from phenylalanine-17 to phenylalanine-28 of a yeast mitochondrial ATPase inhibitor is essential for its ATPase inhibitory activity, *J Biochem.* **130**, 687-93.
14. Rouslin, W. (1988) Factors affecting the loss of mitochondrial function during zero-flow ischemia (autolysis) in slow and fast heart-rate hearts, *J Mol Cell Cardiol.* **20**, 999-1007.
15. Campanella, M., Casswell, E., Chong, S., Farah, Z., Wieckowski, M. R., Abramov, A. Y., Tinker, A. & Duchen, M. R. (2008) Regulation of mitochondrial structure and function by the F_1F_o-ATPase inhibitor protein, IF_1, *Cell Metab.* **8**, 13-25.

16. Formentini, L., Sanchez-Arago, M., Sanchez-Cenizo, L. & Cuezva, J. M. (2012) The mitochondrial ATPase inhibitory factor 1 triggers a ROS-mediated retrograde prosurvival and proliferative response, *Mol Cell.* **45**, 731-42.
17. Sanchez-Arago, M., Formentini, L., Martinez-Reyes, I., Garcia-Bermudez, J., Santacatterina, F., Sanchez-Cenizo, L., Willers, I. M., Aldea, M., Najera, L., Juarranz, A., Lopez, E. C., Clofent, J., Navarro, C., Espinosa, E. & Cuezva, J. M. (2013) Expression, regulation and clinical relevance of the ATPase inhibitory factor 1 in human cancers, *Oncogenesis.* **2**, e46.
18. He, J., Ford, H. C., Carroll, J., Douglas, C., Gonzales, E., Ding, S., Fearnley, I. M. & Walker, J. E. (2018) Assembly of the membrane domain of ATP synthase in human mitochondria, *Proc Natl Acad Sci U S A.* **115**, 2988-2993.
19. Matthews, K. R. (2015) 25 years of African trypanosome research: From description to molecular dissection and new drug discovery, *Mol Biochem Parasitol*.
20. Tielens, A. G. & van Hellemond, J. J. (2009) Surprising variety in energy metabolism within Trypanosomatidae, *Trends Parasitol.* **25**, 482-90.
21. Besteiro, S., Barrett, M. P., Riviere, L. & Bringaud, F. (2005) Energy generation in insect stages of Trypanosoma brucei: metabolism in flux, *Trends Parasitol.* **21**, 185-91.
22. Zikova, A., Hampl, V., Paris, Z., Tyc, J. & Lukes, J. (2016) Aerobic mitochondria of parasitic protists: Diverse genomes and complex functions, *Mol Biochem Parasitol*.
23. Smith, T. K., Bringaud, F., Nolan, D. P. & Figueiredo, L. M. (2017) Metabolic reprogramming during the *Trypanosoma brucei* life cycle, *F1000Res.* **6**.
24. Nolan, D. P. & Voorheis, H. P. (1992) The mitochondrion in bloodstream forms of *Trypanosoma brucei* is energized by the electrogenic pumping of protons catalysed by the F_1F_o-ATPase, *Eur J Biochem.* **209**, 207-16.
25. Schnaufer, A., Clark-Walker, G. D., Steinberg, A. G. & Stuart, K. (2005) The F_1-ATP synthase complex in bloodstream stage trypanosomes has an unusual and essential function, *EMBO J.* **24**, 4029-40.
26. Panicucci, B., Gahura, O. & Zikova, A. (2017) Trypanosoma brucei $TbIF_1$ inhibits the essential F_1-ATPase in the infectious form of the parasite, *PLoS Negl Trop Dis.* **11**, e0005552.
27. Bason, J. V., Runswick, M. J., Fearnley, I. M. & Walker, J. E. (2011) Binding of the inhibitor protein IF_1 to bovine F_1-ATPase, *J Mol Biol.* **406**, 443-53.
28. Greenfield, N. J. (2006) Using circular dichroism spectra to estimate protein secondary structure, *Nat Protoc.* **1**, 2876-90.
29. McDonnell, A. V., Jiang, T., Keating, A. E. & Berger, B. (2006) Paircoil2: improved prediction of coiled coils from sequence, *Bioinformatics.* **22**, 356-8.
30. Gahura, O., Subrtova, K., Vachova, H., Panicucci, B., Fearnley, I. M., Harbour, M. E., Walker, J. E. & Zikova, A. (2018) The F_1-ATPase from *Trypanosoma brucei* is elaborated by three copies of an additional p18-subunit, *FEBS J.* **285**, 614-628.
31. Rouslin, W. (1987) Factors affecting the reactivation of the oligomycin-sensitive adenosine 5'-triphosphatase and the release of ATPase inhibitor protein during the re-energization of intact mitochondria from ischemic cardiac muscle, *J Biol Chem.* **262**, 3472-6.
32. Rouslin, W. & Pullman, M. E. (1987) Protonic inhibition of the mitochondrial adenosine 5'-triphosphatase in ischemic cardiac muscle. Reversible binding of the ATPase inhibitor protein to the mitochondrial ATPase during ischemia, *J Mol Cell Cardiol.* **19**, 661-8.
33. Subrtova, K., Panicucci, B. & Zikova, A. (2015) ATPaseTb2, a unique membrane-bound F_oF_1-ATPase component, is essential in bloodstream and dyskinetoplastic trypanosomes, *PLoS Pathog.* **11**, e1004660.
34. Montgomery, M. G., Gahura, O., Leslie, A. G. W., Zikova, A. & Walker, J. E. (2018) ATP synthase from *Trypanosoma brucei* has an elaborated canonical F_1-domain and conventional catalytic sites, *Proc Natl Acad Sci U S A.* **115**, 2102-2107.
35. Andries, K., Verhasselt, P., Guillemont, J., Gohlmann, H. W., Neefs, J. M., Winkler, H., Van Gestel, J., Timmerman, P., Zhu, M., Lee, E., Williams, P., de Chaffoy, D., Huitric, E., Hoffner, S., Cambau, E., Truffot-Pernot, C., Lounis, N. & Jarlier, V. (2005) A diarylquinoline drug active on the ATP synthase of *Mycobacterium tuberculosis*, *Science.* **307**, 223-7.

456 36. Preiss, L., Langer, J. D., Yildiz, O., Eckhardt-Strelau, L., Guillemont, J. E., Koul, A. & Meier, T. (2015)
457 Structure of the mycobacterial ATP synthase F_o rotor ring in complex with the anti-TB drug bedaquiline,
458 *Sci Adv.* **1**, e1500106.
459 37. Silvester, J. A., Dickson, V. K., Runswick, M. J., Leslie, A. G. & Walker, J. E. (2006) The expression,
460 purification, crystallization and preliminary X-ray analysis of a subcomplex of the peripheral stalk of ATP
461 synthase from bovine mitochondria, *Acta Crystallogr Sect F Struct Biol Cryst Commun.* **62**, 530-3.
462 38. Miroux, B. & Walker, J. E. (1996) Over-production of proteins in *Escherichia coli*: mutant hosts that
463 allow synthesis of some membrane proteins and globular proteins at high levels, *J Mol Biol.* **260**, 289-98.
464 39. Pullman, M. E., Penefsky, H. S., Datta, A. & Racker, E. (1960) Partial resolution of the enzymes
465 catalyzing oxidative phosphorylation. I. Purification and properties of soluble dinitrophenol-stimulated
466 adenosine triphosphatase, *J Biol Chem.* **235**, 3322-9.
467 40. Claros, M. G. & Vincens, P. (1996) Computational method to predict mitochondrially imported proteins
468 and their targeting sequences, *Eur J Biochem.* **241**, 779-86.
469 41. Cole, C., Barber, J. D. & Barton, G. J. (2008) The Jpred 3 secondary structure prediction server, *Nucleic*
470 *Acids Res.* **36**, W197-201.
471 42. Edgar, R. C. (2004) MUSCLE: multiple sequence alignment with high accuracy and high throughput,
472 *Nucleic Acids Res.* **32**, 1792-7.
473

474 **Supporting information:**

475 Table S1: Intact molecular masses of $TbIF_1$ and its variants

476 Table S2: Interactions between amino acids in subunits of bovine F_1-ATPase and bovine IF_1 and their

477 possible conservation in *T. brucei*

478 Table S3: List of oligonucleotides

479 Figure S1: Analysis of kinetic data illustrated with the example of $TbIF_1$-WT at pH 8.0

TABLES

TABLE 1. Oligomerization of $TbIF_1$

Apparent molecular weights were determined by size exclusion chromatography on Superdex 75.

Protein	pH	Molecular weight		Oligomerization state
		Calculated	Measured	
$TbIF_1$-WT	8.0		44.5	Dimer
	7.4	12.3	42.8	Dimer
	6.5		38.2	Dimer
$TbIF_1$(1-64)	8.0		18.9	Monomer
	7.4	8.7	18.5	Monomer
	6.5		18.2	Monomer
bovine IF_1	8.0	10.4	79.0	Tetramer
bovine I1-60	8.0	7.6	16.4	Monomer

485 **TABLE 2. Kinetic parameters of inhibition of F_1-ATPase by $TbIF_1$**

Inhibitor protein	pH	k_{on} (10^{-2} $\mu M^{-1}s^{-1}$)	k_{off} (10^{-4} s^{-1})	K_i (10^{-2} μM)
$TbIF_1$	8.0	2.2±0.51	44±14	18.3±3.9
	6.5	5.1±0.81	4.2±0.30	0.64±0.20
$TbIF_1$(1-64)	8.0	1.9±0.08	35±23	17.9±1.8
	6.5	6.0±2.7	2.8±0.47	0.52±0.10

486

487

FIGURES

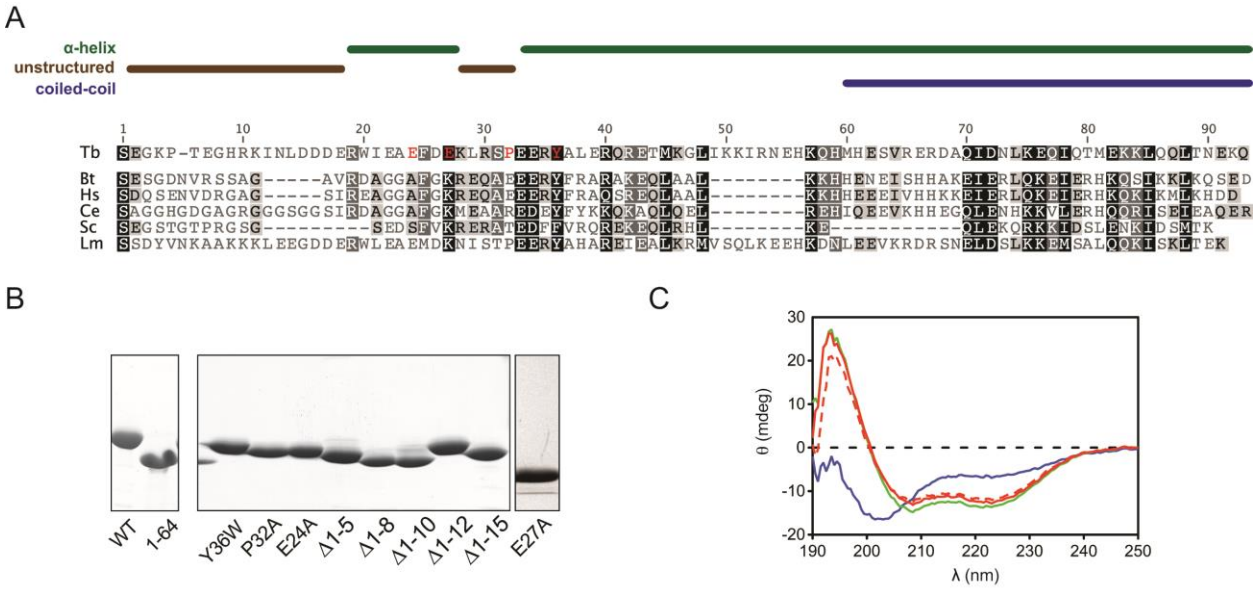

FIGURE 1. **(A) Predicted secondary structure of $TbIF_1$ and conservation of IF_1 sequences from various species.** $TbIF_1$ has not been characterized from a native source, and therefore the exact point where the mitochondrial import precursor is cleaved is not known experimentally. However, the cleavage site is predicted to occur following residue 22 of the precursor making serine 23 of the precursor to be residue 1 of the mature protein. The numbering of the mature protein is used in this figure. The secondary structure was predicted with Jpred [41], and regions with the capacity to form α-helical coils were predicted with Paircoil2 [29]. In this study, truncated versions of $TbIF_1$ with residues 1-5, 1-8, 1-10, 1-12 and 1-15 deleted are described. In other forms of $TbIF_1$ specific residues (red) were mutated to alanine and Tyr-36 was mutated to tryptophan. The alignment of the sequences of $TbIF_1$ with inhibitor proteins from other species was generated with MUSCLE [42]. The similarities of residues highlighted in black, dark grey, and light grey as calculated with the Blossum 62 scoring matrix and threshold set to 1 are 100%, <100% and ≥80%, and <80% and ≥60%, respectively. *Lm, Leishmania major; Tb, Trypanosoma brucei; Sc, Saccharomyces cerevisiae; Ce, Caenorhabditis elegans; Bt, Bos taurus; Hs, Homo sapiens*.

(B) Analysis of purified of TbIF1 and variants by SDS-PAGE. The gel was stained with Coomassie Blue dye. **(C) Circular dichroism spectra of $TbIF_1$ variants**. $TbIF_1$-WT, red; $TbIF_1$(1-64), blue;

TbIF$_1$(P32A), green. Each spectrum was recorded four times at pH 6.5 (solid lines) or pH 8.0 (dashed red line) and the resulting averaged profiles are shown.

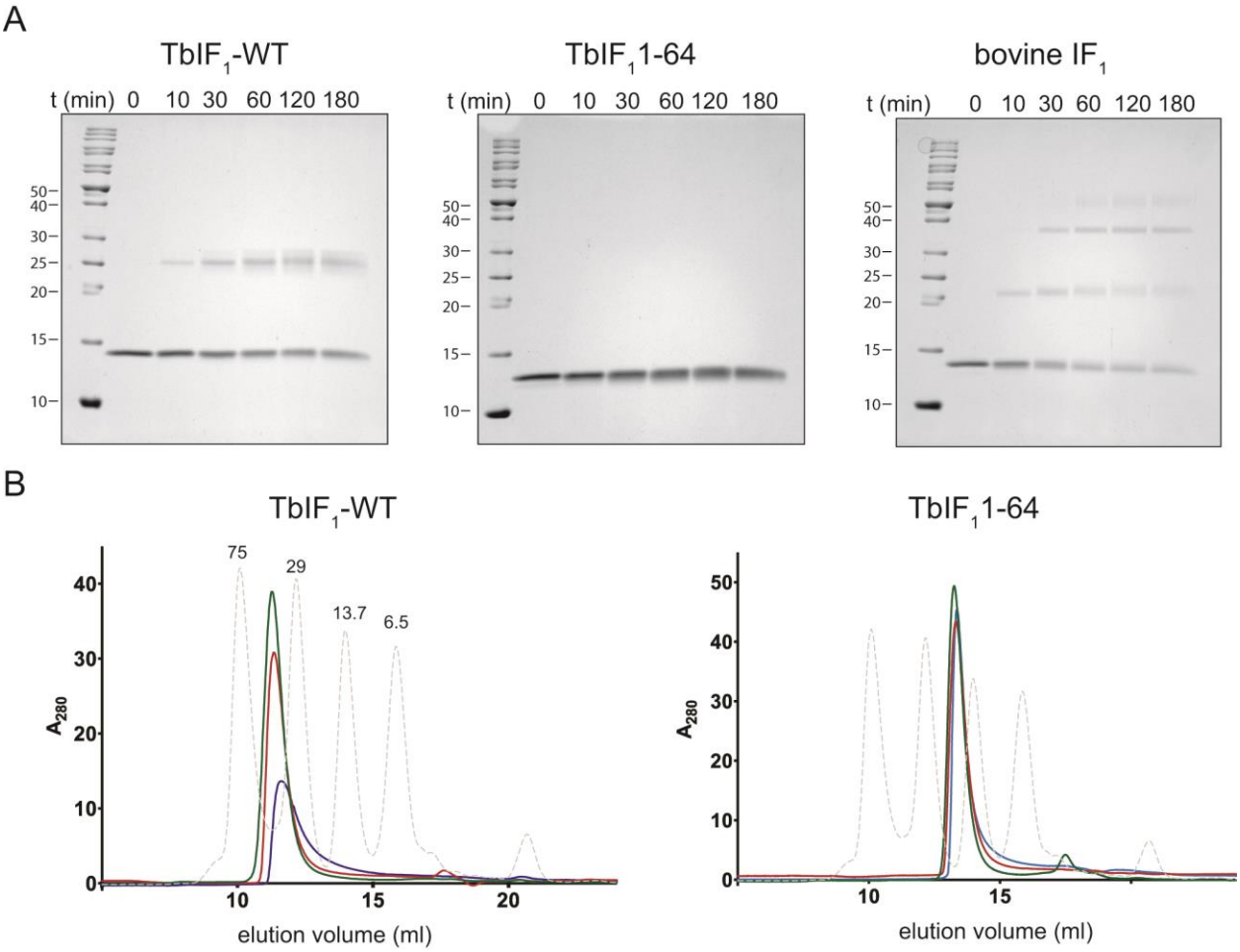

FIGURE 2. **(A) Covalent cross-linking of TbIF$_1$.** TbF$_1$-WT, TbIF$_1$(1-64) and bovine IF$_1$ were cross-linked with dimethylsuberimidate and analysed by SDS-PAGE on 15% polyacrylamide gels. The proteins were stained with Coomassie blue dye. The duration of the cross-linking reaction is indicated above the gels. (B) **Size exclusion chromatography of TbIF$_1$-WT and TbIF$_1$(1-64).** The size exclusion chromatography was performed at pH 8.0 (green line), 7.4 (red line), and 6.5 (blue line). Molecular weights of standard proteins are indicated above the respective positions in their elution profile (grey dashed line).

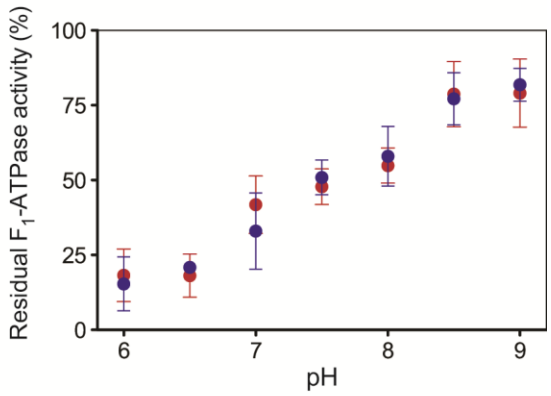

514

515 FIGURE 3. **Effect of pH on the inhibitory activities of $TbIF_1$ (red) and $TbIF_1$(1-64) (blue) on F_1-**
516 **ATPase.** The error bars represent the standard deviations from three independent experiments. TbIF1 was
517 present at least at 30-molar excess over F_1-ATPase.

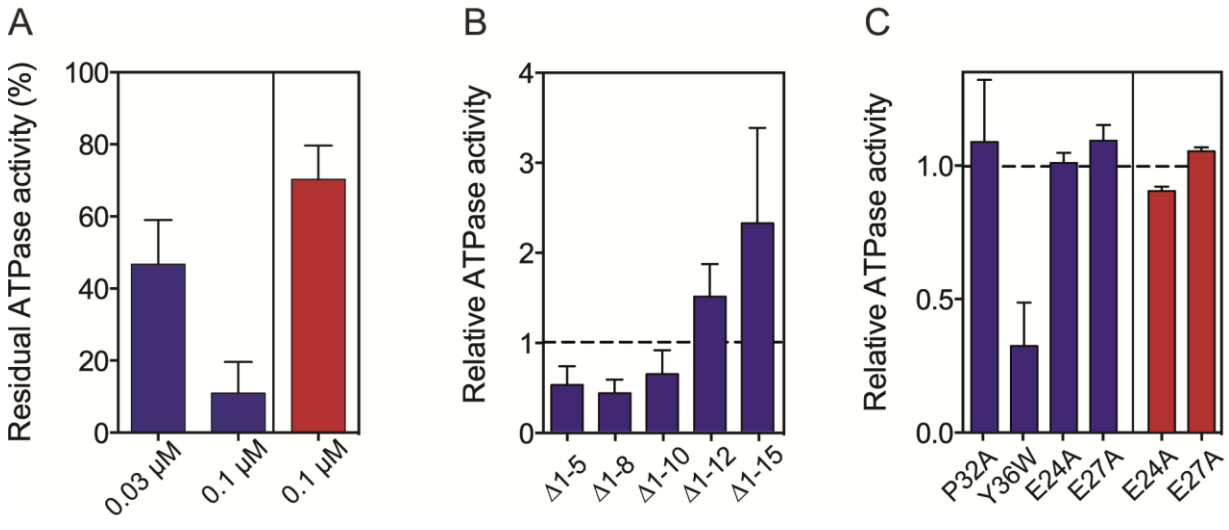

518

519 FIGURE 4. **Effects of N-terminal truncation and point mutations on the inhibitory capacity of $TbIF_1$.**
520 Residual activities of F_1-ATPase inhibited in (A) by intact $TbIF_1$ at two concentrations; in (B) by N-
521 terminally truncated versions of $TbIF_1$ at a concentration of 0.03 µM; and in (C), by versions with point
522 mutations at a concentration of 0.1 µM. The experiments were performed at pH 6.5 (blue bars) or 8.0 (red
523 bars). The values in (B) and (C) are normalized to the level of inhibition by $TbIF_1$-WT at the same
524 concentration (dashed lines). Error bars represent the standard deviations from at least three experiments.

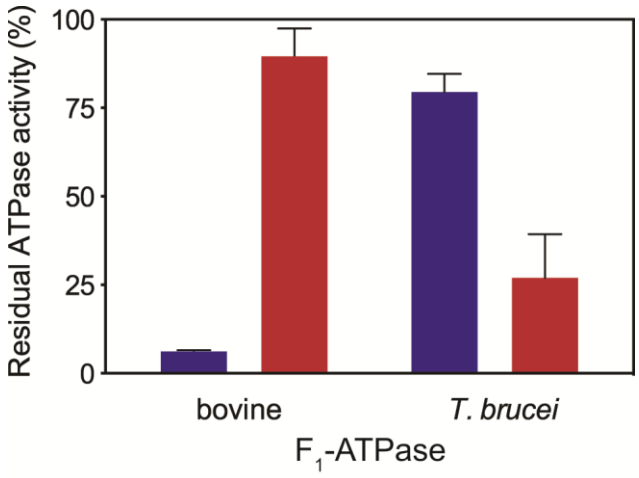

FIGURE 5. **Heterologous inhibition of F_1-ATPase by IF_1.** The F_1-ATPases from *T. brucei* and bovine mitochondria were inhibited with 0.1 μM bovine IF_1 (blue bars) or $TbIF_1$ (red bars). The residual activity was determined at pH 6.5. Error bars represent the standard deviations from two independent experiments conducted in triplicate.